Reorientational Eigenmode Dynamics: A Combined MD/NMR Relaxation Analysis Method for Flexible Parts in Globular Proteins

Jeanine J. Prompers and Rafael Brüschweiler*

Contribution from the Carlson School of Chemistry and Biochemistry, Clark University, Worcester, Massachusetts 01610

Received March 19, 2001. Revised Manuscript Received May 2, 2001

Abstract: An approach is presented for the interpretation of heteronuclear NMR spin relaxation data in mobile protein parts in terms of reorientational eigenmode dynamics. The method is based on the covariance matrix of the spatial functions of the nuclear spin interactions that cause relaxation expressed as spherical harmonics of rank 2. The approach was applied to characterize the dynamics of a loop region of ubiquitin. The covariance matrix was determined from a conformational ensemble generated by a 5 ns molecular dynamics simulation. It was found that the time correlation functions of the dominant eigenmodes decay in good approximation with a single correlation time. From the reorientational eigenmodes, their eigenvalues, and correlation times, NMR relaxation data were calculated in accordance with Bloch−Wangsness−Redfield relaxation theory and directly compared with experimental ^{15}N relaxation parameters. Using a fitting procedure, agreement between calculated and experimental data was improved significantly by adjusting eigenvalues and correlation times of the dominant modes. The presented procedure provides detailed information on correlated reorientational dynamics of flexible parts in globular proteins. The covariance matrix was linked to the covariance matrix of backbone dihedral angle fluctuations, allowing one to study the motional behavior of these degrees of freedom on nano- and subnanosecond time scales.

1. Introduction

To perform their function, proteins often exhibit a significant degree of flexibility and dynamics, which may occur on a wide range of time scales from femtoseconds to seconds. Since flexible parts of globular proteins, such as loop regions and side chains, are often involved in mediating specific protein−protein and protein−DNA interactions, detailed descriptions of the dynamics of these parts and their changes upon establishment of specific contacts should help to obtain a better understanding of biologically important molecular processes. Atoms in biomolecules do not move independently, but rather in a collective fashion. Therefore, a description that takes motional correlation effects into account is desirable.

Much of what is known about rapid biomolecular dynamics stems from nuclear magnetic resonance (NMR) spin relaxation data[1,2] and molecular dynamics (MD) computer simulations.[3] The two methods are complementary:[4] spin relaxation experimentally monitors local reorientational motions of internuclear vectors and their correlation times while MD provides a most detailed theoretical view of protein dynamics.

Most commonly, heteronuclear spin relaxation data of proteins are interpreted on a residue-by-residue basis using the model-free approach,[5−8] spectral density mapping,[9] or analytical motional models.[10,11] The results of such analyses can be directly compared with relaxation parameters calculated from a MD simulation.[12−18] More integrated combinations of MD and NMR relaxation use analytical motional models derived from the trajectory followed by fitting of the model parameters to experimental data,[19−21] the computation of NMR relaxation properties from harmonic and quasiharmonic analyses,[13,22−30] and the jumping-among-minima concept.[31,32]

* To whom correspondence should be addressed. Phone: (508) 793-7220. Fax: (508) 793-8861. E-mail: bruschweiler@nmr.clarku.edu.

(1) Kay, L. E. *Nature Struct. Biol.* **1998**, *5*, 513−517.
(2) Ishima, R.; Torchia, D. A. *Nature Struct. Biol.* **2000**, *7*, 740−743.
(3) Brooks, C. L., III.; Karplus, M.; Pettitt, B. M. *Proteins: A Theoretical Perspective of Dynamics, Structure, and Thermodynamics*; John Wiley & Sons: New York, 1988.
(4) Brüschweiler, R.; Case, D. A. *Prog. NMR Spectrosc.* **1994**, *26*, 27−58.
(5) (a) Lipari, G.; Szabo, A. *J. Am. Chem. Soc.* **1982**, *104*, 4546−4559. (b) Lipari, G.; Szabo, A. *J. Am. Chem. Soc.* **1982**, *104*, 4559−4570.
(6) Clore, G. M.; Szabo, A.; Bax, A.; Kay, L. E.; Driscoll, P. C.; Gronenborn, A. M. *J. Am. Chem. Soc.* **1990**, *112*, 4989−4991.
(7) Kay, L. E.; Torchia, D. A.; Bax, A. *Biochemistry* **1989**, *28*, 8972−8979.
(8) Palmer, A. G.; Rance, M.; Wright, P. E. *J. Am. Chem. Soc.* **1991**, *113*, 4371−4380.
(9) Peng, J. W.; Wagner, G. *Biochemistry* **1992**, *31*, 8571−8586.
(10) Woessner, D. E. *J. Chem. Phys.* **1962**, *36*, 1−4.
(11) Daragan, V. A.; Mayo, K. H. *Prog. NMR Spectrosc.* **1997**, *32*, 63−105.
(12) Levy, R. M.; Karplus, M.; Wolynes, P. G. *J. Am. Chem. Soc.* **1981**, *103*, 5998−6011.
(13) Palmer, A. G.; Case, D. A. *J. Am. Chem. Soc.* **1992**, *114*, 9059−9067.
(14) Chandrasekhar, I.; Clore, G. M.; Szabo, A.; Gronenborn, A. M.; Brooks, B. *J. Mol. Biol.* **1992**, *226*, 239−250.
(15) Kördel, J.; Teleman, O. *J. Am. Chem. Soc.* **1992**, *114*, 4934−4936.
(16) Schmidt, J. M.; Brüschweiler, R.; Ernst, R. R.; Dunbrack, R. L.; Joseph, D.; Karplus, M. *J. Am. Chem. Soc.* **1993**, *115*, 8747−8756. Brunne, R. M.; van Gunsteren, W. F.; Brüschweiler, R.; Ernst, R. R. *J. Am. Chem. Soc.* **1993**, *115*, 4764−4768.
(17) Fushman, D.; Ohlenschläger, O.; Rüterjans, H. *J. Biomol. Struct. Dyn.* **1994**, *4*, 61−78.
(18) Chatfield, D. C.; Szabo, A.; Brooks, B. R. *J. Am. Chem. Soc.* **1998**, *120*, 5301−5311.
(19) Bremi, T.; Brüschweiler, R.; Ernst, R. R. *J. Am. Chem. Soc.* **1997**, *119*, 4272−4284.
(20) Bremi, T.; Brüschweiler, R. *J. Am. Chem. Soc.* **1997**, *119*, 6672−6673.
(21) Lienin, S. F.; Bremi, T.; Brutscher, B.; Brüschweiler, R.; Ernst, R. R. *J. Am. Chem. Soc.* **1998**, *120*, 9870−9879.
(22) Karplus, M.; Kushick, J. *Macromolecules* **1981**, *14*, 325−332.

10.1021/ja0107226 CCC: $20.00
Published on Web 07/06/2001

Collective descriptions of purely reorientational intramolecular motions have recently been developed[33−35] for a comprehensive and yet compact description of correlated dynamics that affect NMR spin relaxation parameters. They rely on the covariance matrices of internuclear vector fluctuations estimated from MD simulations. The methods were used to address contributions of purely reorientational motions of N−H and C−H bonds to the conformational entropy of folded and partially folded protein states in the presence of motional correlations.[34,36]

Nuclear spin relaxation parameters, such as T_1, T_2, and NOE of ^{15}N and ^{13}C spins, are determined by the fluctuations of the angular parts of the lattice functions of the spin-relaxation-active interactions, in particular the magnetic dipole−dipole interaction to directly bonded protons and the chemical shielding anisotropy (CSA) interaction.[37] These lattice functions are commonly represented in terms of spherical harmonics of rank 2, $Y_{2M}(\theta,\varphi)$, where θ,φ are the polar angles describing the orientation of an internuclear vector in a molecule-fixed frame[37] (a non-axially-symmetric CSA interaction can be represented as the sum of two orthogonal axially symmetric interactions[38]). Since relaxation theory by Bloch, Wangsness, and Redfield[39,40] is a second-order perturbation theory, spatial aspects of relaxation properties are completely determined by variance and covariance properties of the $Y_{2M}(\theta,\varphi)$ lattice functions.[41,42]

A generalized interpretation of nuclear spin relaxation data is presented here in terms of a reorientational eigenmode analysis based on the full and a reduced covariance matrix of spherical harmonics $Y_{2M}(\theta,\varphi)$ of different spin-relaxation-active interactions (section 2). The covariance matrix, which is calculated from a MD simulation, is diagonalized yielding reorientational eigenmodes (eigenvectors) and mode amplitudes (eigenvalues) that reflect concerted reorientational motions of the spin interactions that cause relaxation. A characteristic intramolecular correlation time can be assigned to each mode that allows direct calculation of nuclear spin relaxation parameters. Eigenmode amplitudes and correlation times are then adjusted to improve agreement between the experimental and the computed relaxation data. The method is applied in section 3 to study the dynamics of a loop region of the N-terminal β-hairpin of ubiquitin that exhibits increased flexibility.

2. Theory and Methods

General. We consider a molecular dynamics trajectory of a protein of total length T consisting of N conformations (snapshots) sampled with a time increment Δt. We are interested in n dipolar spin−spin interactions, such as ^{15}N−^{1}H and ^{13}C−^{1}H interactions or any other rank 2 interaction, determined by the orientations of their principal axes.[37] A covariance matrix is constructed from the trajectory using the following procedure. First, the six overall motional degrees of freedom are removed by reorienting and translating each conformation by using a least-squares superposition of atomic coordinates with respect to a reference frame, which is for example the conformation at "half-time" $N\Delta t/2$. For each conformation, sampled at time t, the principal axis directions $\Omega_j(t) = (\theta_j(t),\varphi_j(t))$, $j = 1, ..., n$, of the n interactions define the $5n$-dimensional complex column vector:

$$|Y(t)\rangle = |Y_{2,-2}(\Omega_1(t)), Y_{2,-1}(\Omega_1(t)), Y_{20}(\Omega_1(t)), Y_{21}(\Omega_1(t)), Y_{22}(\Omega_1(t)), ..., Y_{2,-2}(\Omega_n(t)), Y_{2,-1}(\Omega_n(t)), Y_{20}(\Omega_n(t)), Y_{21}(\Omega_n(t)), Y_{22}(\Omega_n(t))\rangle \quad (1)$$

where $Y_{2M}(\Omega)$, $M = -2, ..., 2$, are the normalized spherical harmonics of rank 2; $Y_{20}(\theta,\varphi) = c\sqrt{2/3}(3\cos^2\theta - 1)$, $Y_{2,\pm1}(\theta,\varphi) = 2c\cos\theta\sin\theta\exp(\pm i\varphi)$, $Y_{2\pm2}(\theta,\varphi) = c\sin^2\theta\exp(\pm 2i\varphi)$, where $c = \sqrt{15/(32\pi)}$.

The *full* $5n \times 5n$ *covariance matrix* $\boldsymbol{P}$ is then calculated as

$$\boldsymbol{P} = \overline{|\Delta Y\rangle\langle\Delta Y|} \quad (2)$$

where $|\Delta Y\rangle = |Y(t)\rangle - |\bar{Y}\rangle$, with the horizontal bar indicating an ensemble (or time) average over the N conformations of the trajectory, and $\langle\Delta Y|$ is the complex-conjugate row vector to $|\Delta Y\rangle$. Thus, the individual elements of $\boldsymbol{P}$ are of the form

$$P_{iM,jM'} = \overline{|Y_{2M}(\Omega_i) - \overline{Y_{2M}(\Omega_i)}\rangle\langle Y_{2M'}(\Omega_j) - \overline{Y_{2M'}(\Omega_j)}|} \qquad i, j = 1, ..., n \text{ and } M, M' = -2, ..., 2 \quad (3)$$

Matrix $\boldsymbol{P}$ is hermitian ($\boldsymbol{P} = \boldsymbol{P}^\dagger$) and can be diagonalized,

$$\boldsymbol{P}|p\rangle = \lambda_p|p\rangle, \quad p = 1, ..., 5n \quad (4)$$

where $|p\rangle$ are normalized eigenvectors and λ_p are the eigenvalues. The non-zero elements of eigenvector $|p\rangle$ represent the $Y_{2M}(\Omega_j)$ functions that are modulated in a correlated way. Eigenvectors $|p\rangle$ therefore represent the *eigenmodes of reorientation* in rank 2 space with *mode amplitudes* λ_p. The modes are sorted throughout this paper with respect to their amplitudes λ_p, which are all non-negative real numbers, with λ_1 being the smallest amplitude. The non-negativity is due to the fact that the eigenvalues correspond to variances of spherical harmonics along the eigenmodes.

For a molecular ensemble in an isotropic liquid, nuclear spin relaxation does not reflect the individual covariance elements of $\boldsymbol{P}$, but rather the partial traces (see, e.g., ref 4):

$$M_{ij} = \sum_{M=-2}^{2} \overline{|\Delta Y_{2M}(\Omega_i)\rangle\langle\Delta Y_{2M}(\Omega_j)|} = \sum_{l=0}^{4} P_{5i-4+l,5j-4+l} \quad (5)$$

which leads to the *reduced* $n \times n$ *covariance matrix* $\boldsymbol{M}$. Alternatively, $\boldsymbol{M}$ can be expressed as an ensemble average,

(23) Levy, R. M.; Karplus, M.; Kushick, J.; Perahia, D. *Macromolecules* **1984**, *17*, 1370−1374.
(24) Hayward, S.; Kitao, A.; Hirata, F.; Gō, N. *J. Mol. Biol.* **1993**, *234*, 1207−1217.
(25) Amadei, A.; Linssen, A. B.; Berendsen, H. J. *Proteins* **1993**, *17*, 412−425.
(26) Brüschweiler, R. *J. Am. Chem. Soc.* **1992**, *114*, 5341−5344.
(27) Brüschweiler, R.; Case, D. A. *Phys. Rev. Lett.* **1994**, *72*, 940−943.
(28) Brüschweiler, R. *J. Chem. Phys.* **1995**, *102*, 3396−3403.
(29) Abseher, A.; Nilges, M. *J. Mol. Biol.* **1998**, *279*, 911−920.
(30) Horstink, L.; Abseher, R.; Nilges, M.; Hilbers, C. W. *J. Mol. Biol.* **1999**, *287*, 569−577.
(31) Kitao A.; Hayward, S.; Gō, N. *Proteins* **1998**, *33*, 496−517.
(32) Kitao A.; Wagner, G. *Proc. Natl. Acad. Sci. U.S.A.* **2000**, *97*, 2064−2068.
(33) Lienin, S. F.; Brüschweiler, R. *Phys. Rev. Lett.* **2000**, *84*, 5439−5442.
(34) Prompers, J. J.; Brüschweiler, R. *J. Phys. Chem. B* **2000**, *104*, 11416−11424.
(35) Prompers, J. J.; Lienin, S. F.; Brüschweiler, R. In *Biocomputing: Proceedings of the 2001 Pacific Symposium*; Altman, R. B., Dunker, A. K., Hunter, L., Lauderdale, K., Klein, T. E., Eds.; World Scientific: Singapore, 2001; pp 79−88.
(36) Prompers, J. J.; Scheurer, C.; Brüschweiler, R. *J. Mol. Biol.* **2001**, *305*, 1085−1097.
(37) Abragam, A. *Principles of Nuclear Magnetism*; Clarendon Press: Oxford, 1961.
(38) Werbelow, L. G. In *Nuclear Magnetic Resonance Probes of Molecular Dynamics*; Tycko, R., Ed.; Kluwer: Dordrecht, The Netherlands, 1994; pp 223−263.
(39) Wangsness, R. K.; Bloch, F. *Phys. Rev.* **1953**, *89*, 728−739. Bloch, F. *Phys. Rev.* **1956**, *102*, 104−135.
(40) Redfield, A. G. *IBM J. Res. Dev.* **1957**, *1*, 19−31. Redfield, A. G. *Adv. Magn. Reson.* **1965**, *1*, 1−32.
(41) Brüschweiler, R.; Wright, P. E. *J. Am. Chem. Soc.* **1994**, *116*, 8426−8427.
(42) Homonuclear dipolar relaxation with variable internuclear distances will not be discussed here.

$$\boldsymbol{M} = \overline{\boldsymbol{B}(t)} \tag{6}$$

where $\boldsymbol{B}(t) = (\boldsymbol{A}(t) - \overline{\boldsymbol{A}(t)})(\boldsymbol{A}^{\dagger}(t) - \overline{\boldsymbol{A}^{\dagger}(t)})$ and $\boldsymbol{A}(t)$ is an $n \times 5$ matrix with elements $A_{ij} = Y_{2j}(\Omega_i(t))$ constructed from snapshots taken at time t. $\boldsymbol{M}$ is hermitian and can be diagonalized, $\boldsymbol{M}|k\rangle = \lambda_k|k\rangle$, $k = 1, ..., n$, where $|k\rangle$ are normalized reduced reorientational eigenmodes and λ_k are the (real) eigenvalues that reflect the mode amplitudes.

A correlation coefficient of reorientational dynamics between interactions i and j can be calculated from elements of matrix $\boldsymbol{M}$,

$$r_{ij} = \frac{M_{ij}}{(M_{ii}M_{jj})^{1/2}} \tag{7}$$

Correlation Times of Individual Modes. For each reorientational mode $|p\rangle$ or $|k\rangle$ of the full and the reduced covariance matrix, respectively, a characteristic motional time scale can be determined by projecting each snapshot onto the eigenmode. For the full analysis ($5n$-dimensional case of eq 2) this is accomplished by evaluating the scalar product $a_p(t) = \langle p|\Delta Y(t)\rangle$, whereas for the reduced analysis (n-dimensional case of eq 6) an analogous expression can be derived using the trace metric $a_k(t) = Tr\{|k\rangle\langle k|\boldsymbol{B}(t)\} = \langle k|\boldsymbol{B}(t)|k\rangle$. A time correlation function can then be calculated that provides information about the motional time scale(s) of the corresponding mode $|r\rangle$ ($= |p\rangle$ or $|k\rangle$):

$$C_r(t) = \langle a_r^*(\tau + t)a_r(\tau)\rangle_\tau \tag{8}$$

where the average extends over snapshots sampled during the time interval $\tau = 0 \rightarrow T - t$. If the correlation function decays monoexponentially, the correlation time τ_r associated with mode $|r\rangle$ is determined by[5]

$$\tau_r \cong \frac{1}{C_r(0) - C_r(t \rightarrow T)}\int_0^T (C_r(t) - C_r(t \rightarrow T))\,\mathrm{d}t \tag{9}$$

where $C_r(t \rightarrow T)$ symbolizes the plateau value of $C_r(t)$: $C_r(t \rightarrow T) \cong |\langle a_r(\tau)\rangle_\tau|^2$. Examples of correlation functions of dominant reorientational modes will be shown in section 3.

S^2 Order Parameters and Spectral Densities. The generalized S^2 order parameter of autorelaxation data of Lipari and Szabo[5] can be expressed in terms of variances $\sigma^2_{Y_{2M}}$ of the spherical harmonics of rank 2[41]

$$1 - S^2 = \frac{4\pi}{5}\sum_{M=-2}^{2}\sigma^2_{Y_{2M}} \tag{10}$$

where $\sigma^2_{Y_{2M}} = \langle Y_{2M}Y_{2M}^*\rangle - \langle Y_{2M}\rangle\langle Y_{2M}^*\rangle$. Since matrix $\boldsymbol{P}$ contains $\sigma^2_{Y_{2M}}$ as diagonal elements, S^2 of axis j is

$$1 - S_j^2 = \frac{4\pi}{5}\sum_{u=5j-4}^{5j} P_{uu} \tag{11}$$

When starting from the reduced matrix $\boldsymbol{M}$ (eq 5), further simplification occurs since its diagonal elements are directly proportional to $1 - S_j^2$:

$$1 - S_j^2 = \frac{4\pi}{5}M_{jj} \tag{12}$$

For the full analysis involving matrix $\boldsymbol{P}$, the individual contribution $\delta S^2_{j,p}$ of mode p to $1 - S_j^2$ is obtained by inserting the spectral representation of $\boldsymbol{P}$, $\boldsymbol{P} = \sum_p \lambda_p|p\rangle\langle p|$, into eq 11:

$$\delta S^2_{j,p} = \frac{4\pi}{5}\sum_{u=5j-4}^{5j}\lambda_p(|p\rangle\langle p|)_{uu} \tag{13}$$

Similarly, for the reduced analysis involving matrix $\boldsymbol{M}$ the individual contribution $\delta S^2_{j,k}$ of mode k to $1 - S_j^2$ is

$$\delta S^2_{j,k} = \frac{4\pi}{5}\lambda_k(|k\rangle\langle k|)_{jj} \tag{14}$$

where $\delta S^2_{j,p}, \delta S^2_{j,k} \geq 0$ and $\sum_p \delta S^2_{j,p} = \sum_k \delta S^2_{j,k} \leq 1$ must be fulfilled.

The autocorrelation function of the spin interaction j can be expressed as the overall tumbling factor e^{-t/τ_c}, where τ_c is the correlation time for isotropic overall tumbling, times a weighted sum of intramolecular correlation functions $C_r(t)$, that are normalized $C_r(0) = 1$, belonging to individual modes r:

$$C_j(t) = \mathrm{e}^{-t/\tau_c}\{1 + \sum_r \delta S^2_{j,r}(C_r(t) - 1)\} \tag{15}$$

If $C_r(t)$ is monoexponential, $C_r(t) = \mathrm{e}^{-t/\tau_r}$, as is found to be the case to a good approximation in section 3, then the real part of the spectral density function $J_j(\omega)$ can be obtained analytically by cosine transformation:

$$J_j(\omega) = \int_{-\infty}^{\infty} C_j(t)\cos\omega t\,\mathrm{d}t = \frac{2\tau_c}{1 + \omega^2\tau_c^2} + \sum_r \delta S^2_{j,r}\left(\frac{2\tau_r'}{1 + \omega^2\tau_r'^2} - \frac{2\tau_c}{1 + \omega^2\tau_c^2}\right) \tag{16}$$

where r numbers all modes (p or k) and $\tau_r' = \tau_c\tau_r/(\tau_c + \tau_r)$.

Equation 16 provides a formulation of the spectral density function in terms of principal components $\delta S^2_{j,r}$ of the covariance matrices $\boldsymbol{P}$ and $\boldsymbol{M}$, respectively, and their correlation times τ_r. For the reduced analysis eq 16 becomes identical to the Lipari−Szabo model-free approach (see eq 1 of ref 5a) if only a single interaction ($n = 1$) is considered. Generalization of eq 16 for anisotropic overall tumbling is straightforward.

Calculation of NMR Relaxation Parameters. From the spectral density function of eq 16, T_1, T_2, and NOE relaxation parameters can be calculated in a straightforward manner according to standard relaxation theory of Bloch, Wangsness, and Redfield.[39,40] The longitudinal relaxation rate $1/T_1$ of a ^{15}N spin is given by

$$\frac{1}{T_{1,j}} = \frac{1}{20}\left(\frac{\mu_0}{4\pi}\right)^2\left(\frac{h}{2\pi}\right)^2\gamma_N^2\gamma_H^2\langle r_{NH}^{-3}\rangle^2\{3J_j(\omega_N) + J_j(\omega_H - \omega_N) + 6J_j(\omega_H + \omega_N)\} + \frac{1}{15}\omega_N^2(\Delta\sigma)^2 J_j(\omega_N) \tag{17}$$

where μ_0 is the permeability of vacuum, h is Planck's constant, γ_N, γ_H are the gyromagnetic ratios of ^{15}N and ^{1}H, $\Delta\sigma$ is the chemical shielding anisotropy constant, and r_{NH} is the N−H distance. ω_N and ω_H are the Larmor frequencies (in radians per second) of the ^{15}N and ^{1}H nuclei, respectively. The corresponding expressions for $1/T_2$ and the NOE are

$$\frac{1}{T_{2,j}} = \frac{1}{40}\left(\frac{\mu_0}{4\pi}\right)^2\left(\frac{h}{2\pi}\right)^2\gamma_N^2\gamma_H^2\langle r_{NH}^{-3}\rangle^2\{4J_j(0) + 3J_j(\omega_N) + J_j(\omega_H - \omega_N) + 6J(\omega_H) + 6J_j(\omega_H + \omega_N)\} + \frac{1}{90}\omega_N^2(\Delta\sigma)^2\{4J_j(0) + 3J_j(\omega_N)\} \tag{18}$$

$$\mathrm{NOE}_j = 1 + \frac{\gamma_H}{\gamma_N}T_{1,j}\Gamma_j \tag{19}$$

where $\Gamma_j = (1/20)(\mu_0/4\pi)^2(h/2\pi)^2\gamma_N^2\gamma_H^2\langle r_{NH}^{-3}\rangle^2\{6J_j(\omega_H + \omega_N) - J_j(\omega_H - \omega_N)\}$ is the $^1\mathrm{H} \rightarrow {}^{15}\mathrm{N}$ cross-relaxation rate constant.

The expression for the spectral density function of eq 16 is well-suited for the adjustment of amplitudes λ_r and of correlation times τ_r using a standard nonlinear least-squares fitting procedure (see, e.g., ref 43) to improve the agreement between experiment and theory as is demonstrated in section 3. We call this approach *reorientational*

(43) Press, W. H.; Flannery, B. P.; Teukolsky, S. A.; Vetterling, W. T. *Numerical Recipes in C*; Cambridge University Press: Cambridge, 1988.

eigenmode dynamics (RED) analysis. Cross-correlated relaxation effects can be incorporated similar to autocorrelated relaxation effects (see Appendix).

Restrained Fitting for the Full RED Analysis. In the full RED analysis, the number of modes may exceed the number of experimental parameters and thus the fitting procedure becomes underdetermined. For the sake of conceptual simplicity it is desirable if the modified matrix $\boldsymbol{M}'$, which is calculated from a modified matrix $\boldsymbol{P}' = \sum_p \lambda_p' |p\rangle\langle p|$ using eq 5, where λ_p' are the modified amplitudes, has eigenvectors $|k'\rangle$ that remain essentially unchanged with respect to the original eigenvectors $|k\rangle$. This is accomplished by restricting the fitting to a subspace spanned by the relaxation-active motions. The subspace is defined by the quantities O_{pk} that represent the overlap between the eigenvectors $|p\rangle$ of $\boldsymbol{P}$ and the eigenvectors $|k\rangle$ of $\boldsymbol{M}$:

$$O_{pk} = Tr\{Tr_5(|p\rangle\langle p|)|k\rangle\langle k|\} \tag{20}$$

where $Tr_5(|p\rangle\langle p|)$ denotes the $n \times n$ matrix constructed from $|p\rangle\langle p|$ by forming the partial traces over 5×5 sub-blocks of matrix $|p\rangle\langle p|$. The modified amplitudes λ_p' of $\boldsymbol{P}$ can then be expressed as

$$\lambda_p' = \lambda_p \sum_{k=1}^{n} O_{pk} x_k \tag{21}$$

where x_k, $k = 1, ..., n$, are the n fit parameters. For $x_k = 1$ it follows $\lambda_p' = \lambda_p$. Due to the large number of correlation times τ_p ($p = 1, ..., 5n$), they were used in section 3 as fit parameters only for the largest modes.

Linking RED Modes to Fluctuations of Other Degrees of Freedom. Certain aspects of intramolecular protein motions can sometimes be better visualized in terms of coordinates other than internuclear vectors, for example dihedral angles or distances. Information on the nano- and subnanosecond time scale dynamics of these degrees of freedom offers valuable insights into the motional behavior of the protein and its parts. Such coordinates and their fluctuations may not be directly observable by experiment, but their dynamics properties may be coupled to internuclear vectors and their reorientations. We focus in the following on the treatment of dihedral angle fluctuations, but the concept is applicable to other degrees of freedom as well.

Analytical relationships between spin-relaxation-active motions and dihedral angle fluctuations in macromolecules can be derived under favorable circumstances.[19] If analytical relationships become too complicated, statistical approaches can be used instead.[28,44] In the present context a statistical approach is described that links the covariance matrix $\boldsymbol{P}$ of the relaxation-active motions with the covariance matrix of the dihedral angles of interest via a hybrid covariance matrix between the two sets of degrees of freedom. The full covariance matrix $\boldsymbol{P}$ is preferred here over the reduced matrix $\boldsymbol{M}$, since it involves a larger number of stochastic functions that reveal more specific correlations to other degrees of freedom.

Let us consider n relaxation-active interactions of rank 2 represented by $Y_{2M}(\Omega_i)$ and m dihedral angles α_j, representing for example a set of backbone φ,ψ dihedral angles. The total covariance matrix can then be expressed as

$$\boldsymbol{Q} = \begin{bmatrix} \mathrm{cov}(Y_{2M},Y_{2M}) & \mathrm{cov}(Y_{2M},\alpha) \\ \mathrm{cov}(\alpha,Y_{2M}) & \mathrm{cov}(\alpha,\alpha) \end{bmatrix} \tag{22}$$

where $\mathrm{cov}(Y_{2M},Y_{2M}) = \boldsymbol{P}$ is the $5n \times 5n$ covariance matrix of eq 2 and $\mathrm{cov}(\alpha,\alpha) = |\Delta\alpha\rangle\langle\Delta\alpha|$ is the $m \times m$ covariance matrix of the m-dimensional dihedral angle vector $|\Delta\alpha\rangle = |\alpha(t)\rangle - |\bar{\alpha}\rangle$ extracted from the MD trajectory. The dihedral angles (in units of radians) are expressed in an interval such that $\alpha(t) \in [\bar{\alpha} - \pi, \bar{\alpha} + \pi]$.

The $5n \times m$ matrix $\mathrm{cov}(Y_{2M},\alpha) = |\Delta Y\rangle\langle\Delta\alpha| = (\mathrm{cov}(\alpha,Y_{2M}))^{\dagger}$ contains the covariance elements between the $Y_{2M}(\Omega_i)$ functions and the dihedral angles α_j. It is essential that a sufficiently large number of elements of $\mathrm{cov}(Y_{2M},\alpha)$ differ significantly from zero, i.e., that the $Y_{2M}(\Omega_i)$ functions and the considered dihedral angles α_j are motionally correlated. Obviously, in the absence of correlations between the two sets of parameters, NMR relaxation data do not allow one to gain further insight into the fluctuation properties of the dihedral angles. Matrix $\boldsymbol{Q}$ can be diagonalized, $\boldsymbol{Q}|q\rangle = \lambda_q|q\rangle$, $q = 1, ..., 5n + m$, where $|q\rangle$ are normalized eigenmodes that describe combined motions of $Y_{2M}(\Omega_i)$ and α_j and λ_q are the mode amplitudes. The adjustment of the amplitudes λ_q is in analogy to the full RED analysis performed in a restrained manner. For the calculation of the overlaps O_{qk} between the eigenvectors $|q\rangle$ of $\boldsymbol{Q}$ and the eigenvectors $|k\rangle$ of $\boldsymbol{M}$ only the RED parts of $|q\rangle$ are used, i.e., the first $5n$ elements of each vector, and the overlaps are renormalized such that $\sum_{k=1}^{n} O_{qk} = 1$.

After fitting of the mode amplitudes $\lambda_q \rightarrow \lambda_q'$ to experimental relaxation data, a modified $\boldsymbol{Q}$ matrix can be reconstructed by using the spectral representation $\boldsymbol{Q}' = \sum_q \lambda_q' |q\rangle\langle q|$ from which the modified dihedral angle covariance submatrix $\mathrm{cov}(\alpha,\alpha)'$ can be extracted. In analogy to eq 7, the correlation coefficient $r(\alpha_i,\alpha_j)$ of the fluctuations between dihedral angles α_i and α_j can be readily calculated, before and after adjustments of mode amplitudes:

$$r(\alpha_i,\alpha_j) = \frac{\mathrm{cov}(\alpha,\alpha)_{ij}}{(\mathrm{cov}(\alpha,\alpha)_{ii}\mathrm{cov}(\alpha,\alpha)_{jj})^{1/2}} \tag{23}$$

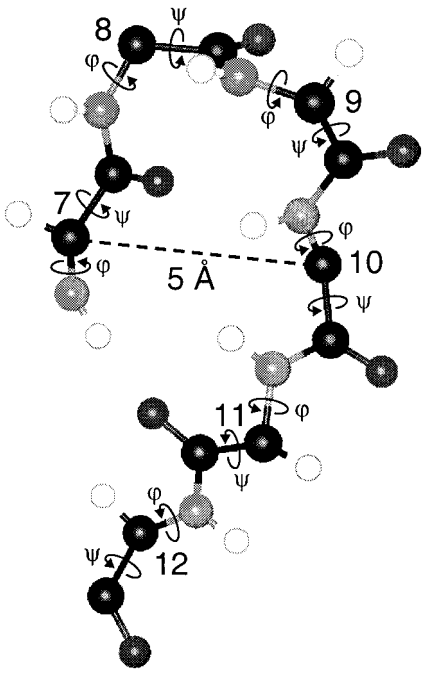

Figure 1. Loop region of the N-terminal β-sheet of ubiquitin consisting of amino acids Thr[7]-Leu[8]-Thr[9]-Gly[10]-Lys[11]-Thr[12] displayed using the VMD software.[45] The coordinates were taken from the conformation at 3.5 ns of the MD trajectory.

3. Application to Loop Dynamics in Ubiquitin

The RED analysis introduced in the previous section was applied to the loop region of the N-terminal β-sheet of the native form of the 76-amino-acid protein ubiquitin. This loop, which is depicted in Figure 1, consists of the amino acid sequence Thr[7]-Leu[8]-Thr[9]-Gly[10]-Lys[11]-Thr[12] and connects the two N-terminal β-strands of ubiquitin. According to both NMR relaxation and MD studies it exhibits enhanced internal mobility.[21,46,47] RED analyses were carried out for both the reduced n-dimensional case and the full $5n$-dimensional case. Further-

(44) LeMaster, D. M. *J. Am. Chem. Soc.* **1999**, *121*, 1726−1742.

(45) Humphrey, W.; Dalke, A.; Schulten, K. *J. Mol. Graphics* **1996**, *14*, 33−38.

(46) Schneider, D. M.; Dellwo, M. J.; Wand, A. J. *Biochemistry* **1992**, *31*, 3645−3652.

(47) Tjandra, N.; Feller, S. E.; Pastor, R. W.; Bax A. *J. Am. Chem. Soc.* **1995**, *117*, 12562−12566.

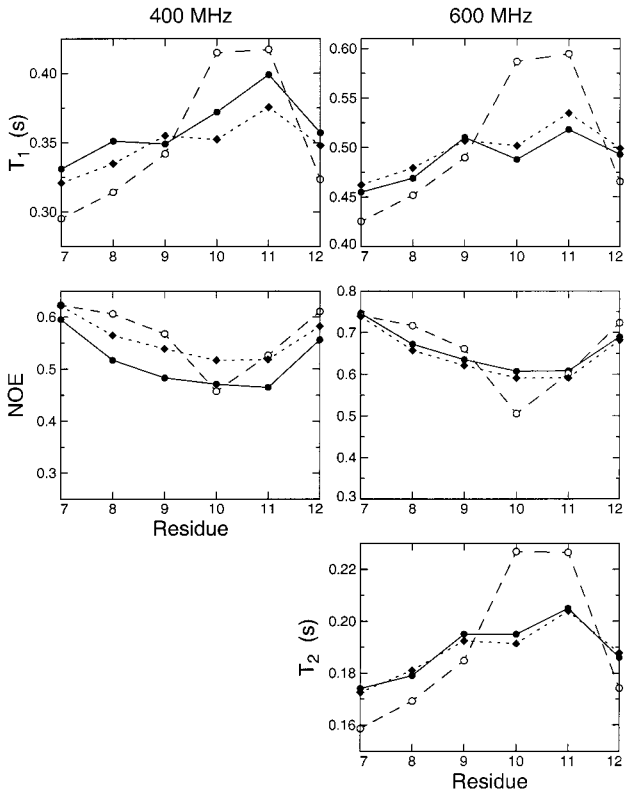

Figure 2. ^{15}N T_1 and T_2 relaxation times and $\{^1$H$\}-^{15}$N NOEs at 600 and 400 MHz proton frequency of loop residues 7−12 of ubiquitin. Experimental relaxation parameters correspond to filled circles. Relaxation parameters calculated using the reduced RED analysis applied to the 5 ns MD trajectory are shown as open circles before fitting, and as filled diamonds after fitting RED amplitudes and correlation times.

more, a combined full RED and dihedral angle fluctuation analysis was performed.

Spin Relaxation Data. Ubiquitin backbone ^{15}N T_1 relaxation times and $\{^1$H$\}-^{15}$N heteronuclear NOEs collected at 400 and 600 MHz and ^{15}N T_2 relaxation times measured at 600 MHz proton frequency were taken from Table 1 of the Supporting Information of Lienin et al.[21] All data were collected at 300 K, and they are shown in Figure 2 as filled circles. According to the ^{15}N relaxation data, this loop is one of the most flexible parts of ubiquitin apart from the C-terminus.[21,46,47] From these data an overall rotational correlation time τ_c of 4.03 ns was determined, which was used for the calculation of relaxation parameters described in the following. Estimates of the statistical uncertainty of the experimental data (standard deviations) that had been obtained by repeating the experiments are[21,48] 1.5% for T_1 values at 400 and 600 MHz, 4% for NOEs at 400 MHz, 2.5% for NOEs at 600 MHz, and 2% for T_2 values at 600 MHz.

MD Simulation of Ubiquitin. An all-atom representation of the protein was embedded in a cubic box including 2909 explicit water molecules, and a 6 ns simulation was carried out under periodic boundary conditions at a temperature of 300 K using the program CHARMM 24.[49,50] A total of 1000 snapshots with a time increment of 5 ps were analyzed from the final 5 ns of the MD simulation. More details about the simulation can be found elsewhere.[21,36] Prior to calculating the covariance matrices, overall translational and reorientational motions were removed

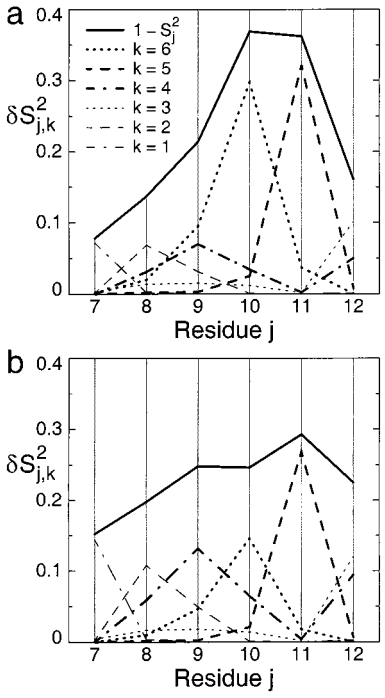

Figure 3. Reorientational mobilities of backbone N−H vectors of the loop residues 7−12 of native ubiquitin expressed in terms of $1 - S_j^2$ values and contributions $\delta S_{j,k}^2$ of reorientational modes $k = 1, ..., 6$ derived from covariance matrix $\boldsymbol{M}$ (eqs 12 and 14). Panels a and b show the reduced RED results before and after optimizing mode amplitudes and correlation times to fit experimental ^{15}N relaxation data.

by a least-squares superposition of the atoms of each snapshot on the ones of the "half-time" snapshot at 3.5 ns.

Residues Thr^7-Leu^8-Thr^9-Gly^{10} of the loop (Figure 1) form a β-turn during the whole trajectory, fluctuating between a type I and a type IV β-turn as classified by the PROMOTIF software.[51] This means that (i) the C$^\alpha$ atoms of residues Thr^7 and Gly^{10} are always within a 7 Å radius and (ii) residues Leu^8 and Thr^9 undergo significant φ,ψ fluctuations while not populating the α region of φ,ψ space.

Reduced RED Analysis. A reduced reorientational eigenmode dynamics analysis was performed on the six N−H vectors of residues 7−12, resulting in six eigenmodes for matrix $\boldsymbol{M}$ (eqs 5 and 6). $1 - S_j^2$ values derived from the diagonal elements of matrix $\boldsymbol{M}$ are plotted in Figure 3a, together with the individual contributions $\delta S_{j,k}^2$ of eq 14 for all six modes $k = 1, ..., 6$. The two largest amplitude modes, modes 5 and 6, predominantly affect residues 11 and 10, respectively, which are the two residues in this loop that exhibit the highest mobility during the MD simulation.

The correlation times of loop motions along the reorientational eigenmodes can be assessed from the autocorrelation functions calculated for each mode using eq 8. The correlation functions $C_k(t)$, which are plotted in Figure 4 for the two largest modes $k = 6$ and $k = 5$, decay in good approximation monoexponentially. Fitting of $C_k(t)$ to $C_k^{\mathrm{fit}}(t) = A \exp(-t/\tau_k)$ yields correlation times $\tau_6 = 56$ ps and $\tau_5 = 38$ ps. These values are in good agreement with the values $\tau_6 = 57$ ps and $\tau_5 = 30$ ps found

(48) Lienin, S. F. *Anisotropic Dynamics in Molecular Systems Studied by NMR Relaxation*; ETH thesis no. 12871; ETH: Zürich, 1998.

(49) Brooks, R. B.; Bruccoleri, R. E.; Olafson, B. D.; States, D. J.; Swaminathan, S.; Karplus, M. *J. Comput. Chem.* **1983**, *4*, 187−217.

(50) MacKerell, A. D., Jr.; Bashford, D.; Bellott, M.; Dunbrack, R. L., Jr.; Evanseck, J. D.; Field, M. J.; Fischer, S.; Gao, J.; Guo, H.; Ha, S.; Joseph-McCarthy, D.; Kuchnir, L.; Kuczera, K.; Lau, F. T. K.; Mattos, C.; Michnick, S.; Ngo, T.; Nguyen, D. T.; Prodhom, B.; Reiher, W. E., III.; Roux, B.; Schlenkrich, M.; Smith, J. C.; Stote, R.; Straub, J.; Watanabe, M.; Wiórkiewicz-Kuczera, J.; Yin, D.; Karplus, M. *J. Phys. Chem. B* **1998**, *102*, 3586−3616.

(51) Hutchinson, E. G.; Thornton, J. M. *Protein Sci.* **1996**, *5*, 212−220.

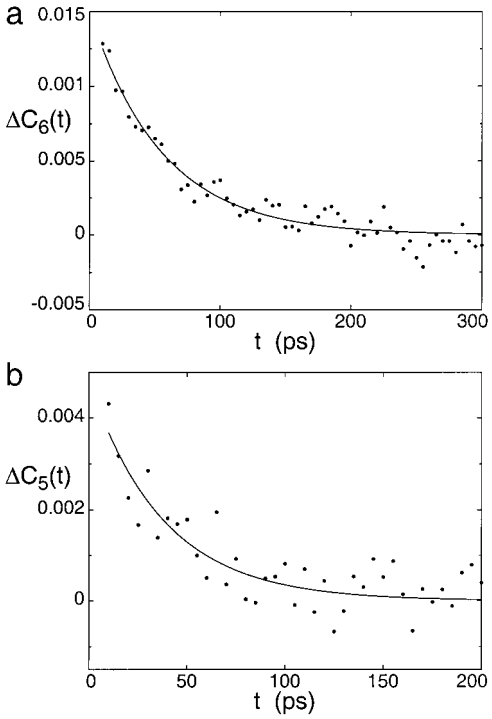

Figure 4. Time correlation functions $\Delta C_k(t) = C_k(t) - C_k(t \rightarrow T)$ of the two largest amplitude reorientational eigenmodes 6 (panel a) and 5 (panel b) of covariance matrix $\boldsymbol{M}$ of loop residues 7−12 calculated using eq 8 (filled circles). Superimposed are monoexponential fits (solid lines).

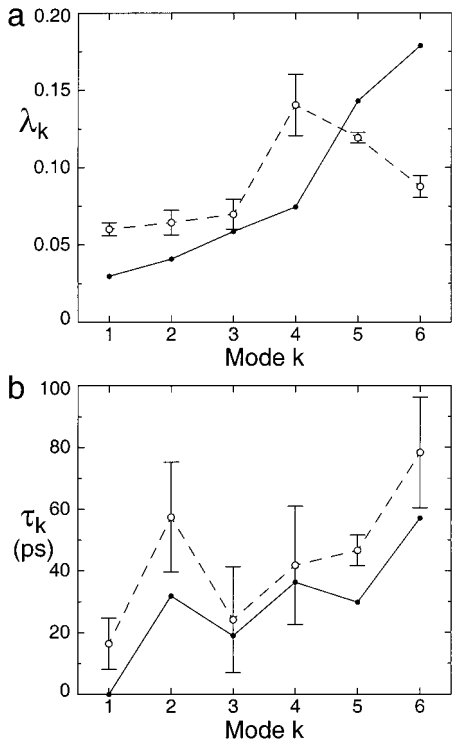

Figure 5. Original (filled circles) and fitted (open circles) reorientational eigenmode amplitudes (panel a) and correlation times (panel b) of the reduced RED analysis applied to the backbone N−H vectors of the loop residues 7−12. The original correlation time of the smallest and fastest mode 1 was set to zero, since it could not be accurately estimated. The error bars were determined by a Monte Carlo error analysis consisting of 100 calculations.

using eq 9. For the smallest amplitude mode, mode 1, the noise present in the time correlation function exceeds the initial value $C_1(0)$, and therefore an effective correlation time could not be accurately determined (see Figure S1 of the Supporting Information).

^{15}N T_1, T_2, and NOE relaxation parameters, shown as open circles in Figure 2, were calculated for the loop residues using the expression for the spectral density of eq 16 with the eigenmodes, amplitudes, and correlation times extracted from the trajectory. Dipolar contributions were included using a N−H bond length of $r_{NH} = 1.02$ Å, and CSA contributions were included using an axially symmetric ^{15}N CSA tensor with the symmetry axis parallel to the N−H vector and with an asymmetry $\Delta\sigma = -160$ ppm. As is seen in Figure 2, the calculated values do not satisfactorily reproduce the experimental relaxation parameters. Hence, amplitudes λ_k and correlation times τ_k of the six eigenmodes were adjusted to better fit the experimental data.

The relaxation parameters corresponding to the best fits are shown in Figure 2 as filled diamonds. The weighted χ^2 improves by a factor of 8 compared to the original MD results, and the agreement between the experimental NMR data and the fitted relaxation parameters, in particular at 600 MHz, becomes remarkably good. The experimental T_1 parameters at 400 MHz display a somewhat different pattern than the 600 MHz parameters that cannot be quantitatively reproduced by the fit. Possible causes are experimental inaccuracies or additional dynamics present in the experiment that is not present in the MD simulation. For the NOE data at 400 MHz, which have a larger experimental uncertainty and therefore a lower weight during the fitting, a small systematic difference between experimental and fitted data remains.

Figure 5 shows the original amplitudes λ_k and intramolecular correlation times τ_k together with the optimized values and their standard deviations calculated from a Monte Carlo error analysis consisting of 100 simulations with the experimental input parameters varied randomly in accordance with their estimated uncertainties. More details on the Monte Carlo error analysis can be found in the Supporting Information (Figure S2). The largest amplitude adjustments are observed for modes 4 and 6 with the amplitude of mode 4 increased and the amplitude of mode 6 decreased. The best-fitting correlation times remain notably close to the correlation times originally extracted from the MD trajectory. The contributions $\delta S^2_{j,k}$ of individual modes k to the order parameters $1 - S_j^2$ are proportional to λ_k and are depicted in Figure 3 for both the original (panel a) and adjusted amplitudes (panel b). After the fitting, residues 7, 8, 9, and 12 have increased mobility as compared to the original MD simulation, whereas residues 10 and 11 have decreased mobility. This leads to a more uniform distribution of mobility along the loop, as can be seen by comparing panels a and b of Figure 3. The fitting also causes a decrease in correlation of reorientational motion between internuclear N−H vectors i and j, which can be expressed according to eq 7 in terms of correlation coefficients r_{ij}: before fitting all $|r_{ij}|$ are 0.39 or lower and after fitting they are 0.25 or lower.

The fitting procedure was repeated using a longer N−H bond length of $r_{NH} = 1.04$ Å proposed recently.[52,53] In this case, a new global minimum is found with significantly longer correlation times for modes 2 and 6 approaching the nanosecond time scale range. If the new correlation times are restricted to a range that is within a factor of 5 or less of the original values, essentially the same minimum is obtained as for the case with

(52) Ottiger, M.; Bax, A. *J. Am. Chem. Soc.* **1998**, *120*, 12334−12341.
(53) Case, D. A. *J. Biomol. NMR* **1999**, *15*, 95−102.

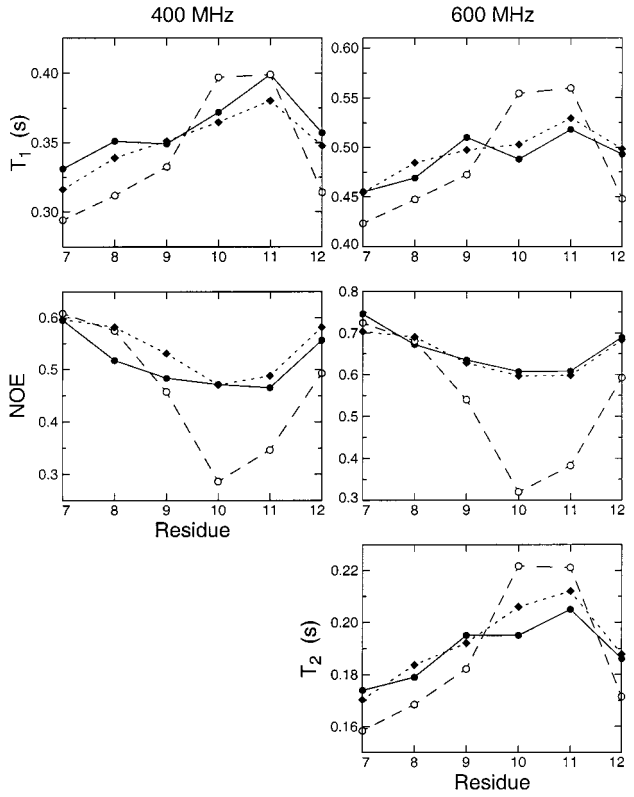

Figure 6. Experimental, back-calculated, and fitted ^{15}N T_1, T_2, and NOE relaxation parameters for the full RED analysis. The same symbols were used as in Figure 2.

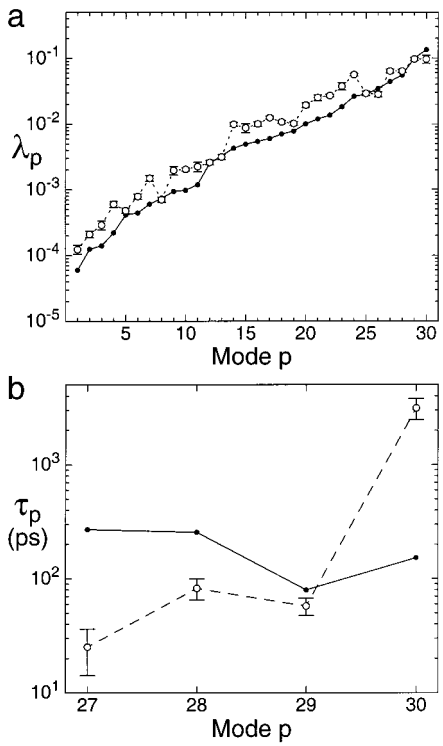

Figure 7. Original (filled circles) and adjusted (open circles) reorientational eigenmode amplitudes (panel a) and correlation times (panel b) of the full RED analysis. The error bars were determined by a Monte Carlo error analysis.

the N−H bond length set to 1.02 Å, but with a systematic offset in the amplitudes and correlation times (see Figures S3 and S4 of the Supporting Information). Since lengthening of the N−H bond reduces the dipolar coupling strength, the fitted mode amplitudes λ_k are decreased while the correlation times τ_k are increased.

Full RED Analysis. A full 5*n*-dimensional RED analysis was performed on the same six N−H vectors of residues 7−12, resulting in 30 eigenmodes for matrix $\boldsymbol{P}$ (eq 2). As described in section 2, $1 - S_j^2$ values derived from $\boldsymbol{P}$ are identical to those derived from $\boldsymbol{M}$, but the individual contributions $\delta S_{j,p}^2$ are now distributed over 30 modes instead of six modes, each with its own correlation time τ_p. A reduction of the number of fitting parameters was achieved by using the restrained fitting procedure of eq 21, which involves only six independent fit parameters to scale the 30 amplitudes λ_p. Since it is not feasible to adjust all 30 correlation times, the correlation times of only the four largest amplitude modes were optimized. These modes have the longest correlation times according to the MD simulation. The correlation times of modes 16−26 were kept at their initial values, while the correlation times of the smallest 15 modes, which contribute only little to the spin relaxation behavior, were assumed to be very short ($\tau_p \ll 10$ ps).

The relaxation parameters calculated from the eigenmodes, amplitudes, and correlation times of the full RED analysis are shown in Figure 6, together with the experimental data. Note that the relaxation parameters calculated prior to fitting differ somewhat from those in Figure 2 due to differences in correlation times: for the reduced analysis all calculated correlation times are shorter than 60 ps, while for the full analysis the four largest modes have correlation times longer than 60 ps, i.e., 270, 255, 80, and 152 ps for modes 27−30, respectively. As a consequence, the back-calculated NOEs for the full RED analysis are lower than those for the reduced RED analysis.

The best fit results of the full RED analysis are shown in Figure 6. Again, good agreement between theory and experiment is achieved. The results are similar to the reduced RED results, where the differences are mainly caused by the distinct treatment of correlation times in the two methods. Figure 7 shows the original amplitudes and intramolecular correlation times together with the optimized values. All 30 amplitudes are scaled using six fit parameters according to eq 21. The amplitudes of the largest modes are hardly changed, while the smaller modes generally have slightly increased amplitudes. The correlation times of mode 28 and especially of mode 27, which are the slowest among all modes, are adjusted to much shorter values. The adjusted correlation time of mode 29 remains very close to its original value. The adjusted correlation time of mode 30 is about 3 ns, which makes this mode essentially NMR relaxation inactive. This mode, which possesses a non-exponential correlation function, is apparently caused by a rare event during the simulation and is not reflected in the experimental NMR spin relaxation parameters.

The full RED analysis yields for this loop results that are comparable to the ones obtained from the reduced RED analysis. However, when correlating vector orientation fluctuations with dihedral angle fluctuations, the full RED approach yields better results, presumably because full RED probes the reorientational fluctuations in a larger variety of different functional forms than reduced RED and allows the occurrence of stronger correlation effects, as is demonstrated in the following section.

Correlating Relaxation with Dihedral Angle Fluctuations. A combined full RED and dihedral angle fluctuation analysis was performed on the six N−H vectors of residues 7−12. The 30 modes of the full RED analysis were correlated with the 12 backbone dihedral angles $\alpha_i = \varphi_7,\psi_7, ..., \varphi_{12},\psi_{12}$, which results

in 42 eigenmodes for the hybrid covariance matrix $\boldsymbol{Q}$ of eq 22. The $1 - S_j^2$ values for the N−H vectors derived from $\boldsymbol{Q}$ are identical to those obtained from matrix $\boldsymbol{M}$ in the reduced analysis. The individual contributions $\delta S_{j,q}^2$ are distributed over 42 modes, each with its individual correlation time. The restrained fitting procedure uses six independent fit parameters to adjust all 42 amplitudes. The correlation times of the five largest modes were individually adjusted during the fitting procedure, and the correlation times of the 27 smallest modes were set to small values ($\tau_q \ll 10$ ps).

The results are very similar to the full RED analysis (see Figures S5 and S6 of the Supporting Information). The largest difference is found for the fitted T_1 and T_2 values for residue 9, which are slightly smaller in the combined analysis. For the fitted mode amplitudes and intramolecular correlation times, the same trends are observed as for the full RED analysis, with the adjusted correlation time of the largest mode, mode 42, being again NMR relaxation inactive ($\tau_{42} = 3-4$ ns).

After fitting, for both the reduced and the full RED analyses, none of the relaxation-active modes (with the exception of mode 30 in the full RED case) exhibits a correlation time exceeding 100 ps. In both cases the longest adjusted correlation time is about 80 ps. In contrast, in the combined analysis mode 38 has an adjusted correlation time of 200 ps. In the full RED subspace this mode mainly affects residue 9, which might explain the differences in the fitted T_1 and T_2 values observed for this residue.

From the adjusted eigenvalues λ_q' an adjusted matrix $\boldsymbol{Q}' = \sum_q \lambda_q' |q\rangle\langle q|$ was determined, which contains the adjusted 12 × 12 covariance submatrix cov(α,α)′ describing the backbone φ,ψ dihedral angle fluctuations and their correlations (see eq 22). Figure 8 shows the φ,ψ root-mean-square fluctuations of residues 7−12 before and after fitting. The φ fluctuations of residues 7, 8, 9, and 12 are slightly increased compared to the original MD simulation, a trend that is similar to the one observed for $1 - S_j^2$ in the reduced RED analysis (Figure 3). The amplitudes of ψ fluctuations remain largely unchanged.

Dihedral angle correlation coefficients were determined according to eq 23 before and after mode amplitude adjustments. The results are summarized in Table 1. Significant correlations between ψ_{i-1},φ_i pairs, which are often found in regular secondary structural elements,[54] are not observed. Before fitting, there are positive correlations involving ψ_8, ψ_9, ψ_{10}, ψ_{11} (all ψ,ψ correlations), and negative correlations involving φ_7, ψ_7, φ_{10}, ψ_{10}, ψ_{11} (all φ,ψ correlations). The highest correlation is observed between ψ_8 and ψ_9, which remains one of the highest correlations also after fitting. Except for the correlation between φ_{10} and ψ_{10}, all other correlations were diminished by the fitting (Table 1), which suggests that the original trajectory tends to overemphasize such correlations. Most affected by the fitting are the positive correlations among ψ dihedral angles, while the negative correlations between φ and ψ dihedral angles are less influenced.

Table 1. Dominant Correlations between Backbone Dihedral Angles

pair of backbone dihedral angles	original correlation coefficients r[a]	correlation coefficients r after adjustments[b]
$\varphi_7-\psi_7$	−0.43	−0.32
$\psi_8-\psi_9$	0.76	0.52
$\psi_8-\psi_{10}$	0.53	0.30
$\psi_9-\psi_{10}$	0.41	0.20
$\varphi_{10}-\psi_{10}$	−0.44	−0.54
$\varphi_{10}-\psi_{11}$	−0.52	−0.45
$\psi_{10}-\psi_{11}$	0.50	0.33

[a] Correlation coefficients of backbone dihedral angles with $|r| \geq 0.4$ according to eq 23, calculated from the original covariance matrix $\boldsymbol{Q}$ of eq 22. [b] Correlation coefficients after optimizing the mode amplitudes and correlation times using the combined full RED and φ,ψ fluctuation analysis.

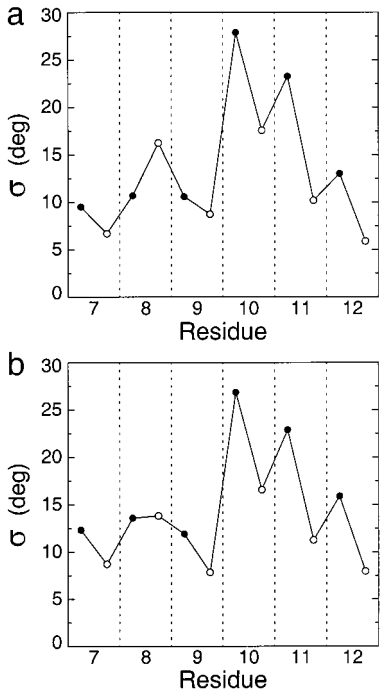

Figure 8. Root-mean-square fluctuations σ of the φ (filled circles) and ψ (open circles) backbone dihedral angles of the loop residues 7−12 of native ubiquitin. Panel a shows the values for the original matrix $\boldsymbol{Q}$ (eq 22), while panel b shows the results after optimizing the mode amplitudes and correlation times using the combined full RED and φ,ψ fluctuation analysis.

4. Conclusion

The short-range character of the spin interactions responsible for NMR relaxation prevents straightforward identification and characterization of correlated protein dynamics from experimental data. The presented RED analysis offers a general solution by combining experimental relaxation data with covariance information extracted from a MD simulation. The covariance matrix is determined from rank 2 spherical harmonics lattice functions Y_{2M} of the nuclear spin interactions that cause spin relaxation. For proteins that can be studied by liquid-state NMR techniques, the NMR relaxation theory of Bloch, Wangsness, and Redfield[39,40] adequately describes nuclear spin relaxation processes. Since this theory is a second-order perturbation theory it involves only second-order time correlation functions of the Y_{2M} functions of the spin interactions. Therefore, the covariance matrix of the Y_{2M} functions represents a complete description of the spatial aspects of protein dynamics that are relevant for nuclear spin relaxation. Third- and higher-order motional correlations have a negligible influence on experimentally observable spin relaxation parameters.

The reorientational covariance matrix is analyzed in terms of its principal components, which are the reorientational eigenmodes and mode amplitudes obtained by matrix diagonalization. It was found that the eigenmodes naturally separate motions occurring on slower and faster time scales, with the slowest modes corresponding to the largest amplitude motions. Thus, the RED modes have a physical meaning in terms of

(54) Levy, R. M.; Karplus, M. *Biopolymers* **1979**, *18*, 2465.

uncoupled reorientational motional modes in analogy to normal modes, quasiharmonic modes, and essential dynamics. The time scale information is used together with the eigenmode and amplitude information to back-calculate relaxation parameters. RED analysis requires only a single MD trajectory and not multiple trajectories that separately sample slow and fast motions.

Back-calculation of spin relaxation parameters is notably simple, since the covariance matrix explicitly comprises S^2 order parameters and thus no conversion of lattice fluctuation amplitudes into S^2 order parameters is necessary. This is in contrast to other collective models of protein motions based on quasiharmonic analysis and essential dynamics. Mode amplitudes of the original covariance matrix and correlation times extracted from the MD trajectory can be readily adjusted by a least-squares fitting procedure to improve agreement with experimental relaxation data.

RED analysis is related to recent approaches for the description of collective reorientational dynamics based on covariance matrices of internuclear vectors expressed in Cartesian coordinates.[33−36] These approaches are mathematically equivalent to the RED analysis if the spherical harmonics of rank 2 are replaced by spherical harmonics of rank 1 (Y_{1M}) to describe the orientations of internuclear vectors.

Since only covariance information of the lattice functions of rank 2 is used, the RED approach is a generalization of the Lipari−Szabo model-free approach[5] to higher dimensions by incorporating effects of concerted motions of different spin interactions on relaxation parameters measured for multiple nuclei. In fact, the diagonal elements of covariance matrix $\boldsymbol{M}$ correspond to $1 - S^2$ while off-diagonal elements represent cross-correlation order parameters. The RED analysis reconciles model-free analysis with quasiharmonic and essential dynamics concepts of protein dynamics for the interpretation of nuclear spin relaxation data. It is particularly suitable for the dynamic characterization of mobile parts of globular proteins such as loop regions and side chains involving a larger number of soft degrees of freedom and whose dynamic parametrization in terms of analytical motional models is hard.

The RED analysis can be coupled to other degrees of freedom, providing an interface between nuclear spin relaxation parameters and the fluctuation properties of these degrees of freedom, as was illustrated here for backbone dihedral angles of ubiquitin. In this way, the MD-derived statistical relationship between backbone φ,ψ fluctuations and reorientational motions of internuclear dipolar vectors combined with experimental relaxation data provides a more accurate characterization of dihedral angle motions on the subnanosecond time scale.

Acknowledgment. J.J.P. is a recipient of a Human Frontier Science Program postdoctoral fellowship. This work was supported by NSF Grant MCB-9904875.

Appendix

Cross-Correlated Relaxation. Cross-correlated relaxation effects between different interactions can be addressed in analogy to autocorrelated relaxation. For the full RED analysis involving matrix $\boldsymbol{P}$, the contribution of mode p to the "decorrelation" of the cross-correlation function between vectors i and j is

$$\delta S^2_{ij,p} = \frac{4\pi}{5}\sum_{u=0}^{4}\lambda_p(|p\rangle\langle p|)_{5i-4+u,5j-4+u} \qquad \text{(A1)}$$

while for the reduced RED analysis involving matrix $\boldsymbol{M}$ the individual contribution of mode k is

$$\delta S^2_{ij,k} = \frac{4\pi}{5}\lambda_k(|k\rangle\langle k|)_{ij} \qquad \text{(A2)}$$

The cross-correlated spectral density function $J_{ij}(\omega)$ that corresponds to eq 16 is obtained by replacing $\delta S^2_{j,r}$ by the corresponding expressions for $\delta S^2_{ij,r}$ from eqs A1 and A2.

Supporting Information Available: Six figures with correlation functions of reduced RED analysis and histograms of Monte Carlo error analysis, results of reduced RED analysis with $r_{NH} = 1.04$ Å, detailed results of the combined full RED and φ,ψ fluctuation analysis (PDF). This material is available free of charge via the Internet at http://pubs.acs.org.

JA0107226